Annales
Geophysicae
Discussions

1 **Analysis of geomagnetic measurements prior the Maule (2010), Iquique (2014) and Illapel (2015)**
2 **earthquakes, in the Pacific Ocean sector of the Southern Hemisphere.**

3 Enrique G. Cordaro (1, 2), Patricio Venegas-Aravena (1, 3, 4) and David Laroze (5, 6).

4 (1) Observatorios de Radiación Cósmica y Geomagnetismo. Dep. Física, F. C. F. M. Universidad de Chile, Casilla 487-
5 3, Santiago, Chile.
6 (2) Facultad de Ingeniería. Universidad Autónoma de Chile. Pedro de Valdivia 425. Santiago. Chile
7 (3) Departamento de Geofísica Universidad de Chile, Blanco Encalada 2002, Santiago, Chile.
8 (4) Department of Structural and Geotechnical Engineering, School of Engineering, Pontificia Universidad Católica de
9 Chile, Vicuña Mackenna 4860, Macul, Santiago, Chile.
10 (5) Instituto de Alta Investigación, CEDENNA, Universidad de Tarapacá, Casilla 7D, Arica, Chile.
11 (6) School of Physical Sciences and Nanotechnology, Yachay Tech University, 00119 Urcuquí, Ecuador.
12
13 E. G. Cordaro: ecordaro@dfi.uchile.cl
14 P. Venegas- Aravena: patricio.venegas@ing.uchile.cl
15 D. Laroze: dlarozen@uta.cl
16

17 **ABSTRACT**
18
19 It has been possible to detect variations in the vertical component of the geomagnetic field (Bz) through its first and
20 second derivate in a range of frequencies (μHz); these seem to be roughly related with some major seismic subduction
21 events. We studied the period 2010-2015, analysing the daily values of magnetic records over periods close to the
22 last three significant events that occurred through the Chilean margin, i. e., along a boundary between convergent
23 plates that is characterized by the occurrence of seismic events of magnitude greater than Mw8. These are the events
24 of Iquique 2014, Illapel 2015 and Maule 2010, all at different latitudes, on different dates and characterized by
25 different types of margin (erosive or accretionary). Certain similarities were found in the associated magnetic field
26 variations: 1) Variation in the radial or z component of the geomagnetic field and its first and second temporal
27 derivative, modelled as a small jump, and small oscillations in the second derivative, generating a frequency band
28 between 1c / 48.9 hours and 1c / 79.13 Hrs. 2) A variable time lapse of between 30 and 120 days; and 3) The seismic
29 event. Furthermore, when analysing spectrograms for the second temporal derivate of the radial component,
30 different behaviour is found related to its spectral density. This takes the form of an increase in ultra-low frequencies
31 (0.01-0.4 mHz) between the start of the magnetic jump and the seismic event. These frequencies are lower than those
32 found during the last years by research groups that related magnetic field and earthquakes, furthermore the concept
33 of time lapse close to 30 days is in agreement with those research groups. The previous analyses may not be so robust,
34 this is why additionally a new method is used with stations closer to the events and time periods of two years. We
35 analysed the daily cumulative number of anomalous behaviour in z component of magnetic field on ground based
36 magnetometers. The results show an increase in the number of magnetic anomalies prior to the occurrence of the
37 three earthquakes. The behavior of the anomalies is similar to those presented by other authors for other
38 earthquakes with similar methods in ionosphere. All this magnetic features might recover seismic information of the
39 events and could be related with Lithosphere-Atmosphere-Ionosphere Coupling.
40
41 Keywords: Geomagnetism, South Atlantic Magnetic Anomaly, Lithosphere-Atmosphere-Ionosphere Coupling,
42 Tectonic plates, Earthquakes

42

43 **1.-Introduction.**

44 The object of this paper is to show the most significant characteristics of the magnetic field and its possible relation
45 with the last three Chilean earthquakes. Specifically, we used the B_z component recorded in the Putre (OP), Easter or
46 Pascua Island (IPM), Osorno (OSO) and Pilar (PIL) observatories. Cordaro et al., 2018, 2019 showed that the variations
47 of the geomagnetic cutoff rigidity (magnetic shielding against the solar wind) have some relation with the Chilean
48 convergent margin. Furthermore, Cordaro et al. (2018) showed that the frequencies of the micro hertz order in the
49 vertical magnetic field also could have some relationship with the earthquake of Maule 2010 Mw8.8. However,
50 Vallianatos and Tzanis (2003) showed that the magnetic field frequencies possibly related to earthquakes comprise a
51 range of at least three orders of magnitude. The last researches have corroborated that the magnetic coupling of
52 ionosphere-lithosphere-atmosphere is statistically related to some earthquake events through variations in the earth
53 magnetic field detected for one month before the seismic events in the frequency range of 5-100 mili-Hertz
54 [Hayakawa and Molchanov, 2002, Pulinets and Boyarchuk, 2004, Varotsos, 2005, Balasis and Mandea 2007,
55 Molchanov and Hayakawa, 2008, Liu, 2010, Hayakawa et al., 2015, Contoyiannis et al., 2016, Potirakis et al., 2016, De
56 Santis et al., 2017, Oikonomou et al., 2017, Marchetti and Akhoondzadeh, 2018, Potirakis et al., 2018] fulfilling the

1   three orders of magnitude in the frequency of the magnetic field proposed by Vallianatos and Tzanis (2003). In
2   consequence, in this paper we focus in the geomagnetic activity before three of strongest earthquakes that hit the
3   Chilean margin during the last years: Maule 2010 (Mw8.8), Iquique 2014 (Mw8.2) and Illapel 2015 (Mw8.3).

4   For other hands, events on the Chilean margin of magnitude greater than Mw8 are generally associated with
5   subduction events, while smaller events are considered of minor interest, and could even be triggered by other
6   events. An example is the event of March 11, 2010 (Mw7), which was a reactivation of the Pichilemu deep intra-plate
7   fault [Farías et al., 2011]. Despite the specific detailed characteristics of the northern and southern parts of the Chilean
8   margin, all events are triggered by small variations or disturbances in stress, allowing stress to fall and energy to be
9   released [Ranjith and Rice, 1999, He et al., 2003].
10
11   Under these conditions, we will study the Chilean territory by examining the variations in the first and second
12   derivative of the Bz component of the magnetic field and the variations in seismic movements produced in the region.
13   We use lower frequencies, longer time series and methods that are different from the ones which have been
14   previously used [Contoyiannis et al., 2016, Potirakis et al., 2016, De Santis et al., 2017, Oikonomou et al., 2017,
15   Marchetti and Akhoondzadeh, 2018]. That is, the Fourier analysis in the range of micro hertz for daily averages values
16   and the Spectrograms method in the range of mili Hertz per minute values. Conceptually, the second derivative of B
17   indicates a change in secular acceleration, which we will call a *jump*. We also introduce the daily cumulative numbers
18   of anomalous behaviour in the component z of magnetic field over the surface of Earth, in the lithosphere. Similar
19   ideas were proposed by De Santis et al. (2017) and by Marchetti and Akhoondzadeh (2018) for Nepal 2015 Mw7.8
20   and Mexico 2017 Mw8.2 earthquakes respectively. In the method applied to the lithosphere we identify the magnetic
21   records with less external disturbances, the variations of the surplus records are considered of lithospheric origin.
22

23   In section 2 we introduce some of the scientific efforts related to magnetism and seismic events. We were able to use
24   the radial component of the magnetic field, its first derivative or secular variation and its second derivative or secular
25   acceleration to try to answer the question as to the origin of the highest-energy seismic movements and look for a
26   possible precursor in section 2.1. In order to do this, we developed an experimental procedure based on the
27   geomagnetic data for three of the most intense seismic events of the South Pacific region: the 2010 Maule
28   earthquake, the 2014 Iquique earthquake and the 2015 Illapel earthquake, all in Chile.
29

30   In section 3 we introduce some manifestation of Space climate in the geomagnetic field during the periods concerned
31   is defined by the Kp magnetic activity index for the months previous to the three earthquakes: Maule 2010 (Dec 15,
32   2009 to Mar 15, 2010), Iquique 2014 (Jan 1, 2014 to Apr 15, 2014) and Illapel 2015 (Jul 1, 2015 to Sep 30, 2015).
33

34   In the section 4 we present an additional methodology using the daily cumulative number of Bz anomalies on Earth
35   surface. Here we use different stations: OSO, with |Dst| <10 nT for the Maule earthquake, and PIL station with |Dst|
36   < 5 nT for the Iquique and Illapel earthquakes. Using quiet times for a period of two years for each earthquake. Finally,
37   we present discussion and conclusions in section 5.
38
39
40   **2. Magnetic field and Seismology.**
41   **2.1. Observatories of geomagnetic data and Magneto-seismic relation.**
42

43   The great majority of studies of the magnetic field and seismic events have been carried out relating temporal
44   variations in the geomagnetic field with frequencies which are comparable to variations in the ionosphere, the space
45   medium and human activity ($0.01 - 10\ Hz$). Besides, they have required specific chemical and geological conditions
46   in fault zones, which restrains the arguments of such studies as they cannot establish any sort of causal mechanism
47   [Thomas et al., 2009a, Thomas et al., 2009b, Thomas et al., 2012, Love and Thomas, 2013, Scoville et al., 2015]. We
48   used the first and second derivatives of the B_z component in the Putre and Ester Island (IPM) station magnetometers,
49   which have not been thoroughly investigated.

50   A high correlation between the vertical component of the earth's magnetic field and seismic activity at the Putre
51   station was found. We therefore seek to specify this behaviour in a shorter time window than the period studied
52   previously (1955-2010). We consider the most significant events that have occurred in recent years in the network of
53   observatories, given their proximity to the Chilean convergent margin and the quality of the data. We start with an
54   analysis of the behaviour of the space medium and its influence on measurements.
55
56   We obtained the values of secular variations in the magnetic field from the Putre (OP), Los Cerrillos (OLC) and Easter
57   Island (IPM) observatories. (Note that the IPM station was closed in 1968 and subsequently reactivated in 2008 by
58   the French INTERMAGNET Group and the Meteorological Service of Chile) [Chulliat et al., 2009, Soloviev et al., 2012].
59

1   The Putre observatory (OP) is at 18°11'47.8S, 69°33'10.9W, 3,598 m.a.s.l (meters above sea level); Los Cerrillos (OLC)
2   is at 33°29'42.3S, 70°42'59.8W, 570 m.a.s.l. They are both located on the western edge of the South American Plate,
3   1,700 kilometres apart from each other. This zone includes the South Atlantic Magnetic Anomaly (SAMA), the centre
4   of which is 1,700 kilometres east of these two observatories, forming an equilateral triangle. IPM is located at 27.1°S,
5   109.2W, 82,83 m.a.s.l, on the western edge of the Nazca plate, characterised as a hotspot [Vezzoli and Acoocella,
6   2009]. OSO is located in the coordinates 40°20'24"S, 74°46'64"W and PIL at 31°40'00.0"S, 63°53'00.0"W.

8   In the Putre and Los Cerrillos observatories, a diminution in the values of the whole magnetic field and each of its
9   components is found. This can be attributed to the fact that the OLC and OP observatories are influenced by the South
10 Atlantic Magnetic Anomaly, while on Easter Island the influence of SAMA is weaker [Storini et al., 1999].

12 The scientific and technical characteristics of the Putre (OP) and Los Cerrillos (OLC) observatories, i.e. location,
13 altitude, atmospheric depth, type of detectors, geomagnetic cutoff rigidities and operating times, may be found in
14 [Cordaro et al., 2012, Cordaro et al., 2016] while for Easter Island (IPM) the information is available in SuperMag
15 Network [Chulliat et al., 2009, Gjerlov, 2012]. The main characteristics for the observatories as location, altitude,
16 atmospheric depth, type of detector, and operations time, are shown in Table 1.

19 The first significant property in the secular variation of the geomagnetic field is determined by the shielding it
20 exercises on the cosmic ray particles which reach the Earth, called the geomagnetic cutoff rigidity. It is defined as the
21 product of the force of the magnetic field and the curvature radius of the incident particle r_g, which relates the
22 geomagnetic latitude with the classification of the particle trajectories and could be related to geological features in
23 the Chilean margin [Pomerantz, 1971, Shea and Smart, 2001, Smart and Shea, 2005, Cordaro et al., 2018, Cordaro et
24 al., 2019].

26 The variations shown during the period 1955-2010 which can explain the non-performance of the latitude effect
27 [Pomerantz, 1971] are of internal origin [Bloxham, 2002, McFadden, 2007, Sarson, 2007, Finlay, 2007]. 3D models of
28 core mantle boundary (CMB) topology based on the velocities of seismic waves [Simmons et al., 2010] show the
29 existence of positive topography in upthrust regions and negative topography in subduction zones [Lassak et al., 2010,
30 Soldati et al., 2012, Yoshida, 2008].

32 It must also be remembered that the intensity of the geomagnetic field at the surface varies between 20,000 and
33 60,000 x 10^{-9} T (from the equatorial zone to the Antarctic in the Pacific Antarctic Sector of the southern hemisphere),
34 and that within the outer core it is estimated to be of the order of 2-4 mT (rms) [Olson, 1999, 2015], thus by focusing
35 attention on measurements of the geomagnetic field (B, B' and B''), evidence can be found of a possible pattern in
36 component B_z in the highest-energy seismic events (Mw > 8.0) occurring in subduction zones during the period 2005-
37 2011, i.e.:. The pattern of the B_z component consists of a jump of the order of 100-300 nT for B , its first temporal
38 change of B as B'_z and its second temporal change of B as B''_z and a time lapse between the jump and the seismic
39 event of the order of 30 to 120 days. This was accompanied by variations in the geomagnetic field with frequencies
40 in the range of 3 to 5 micro Hz, which are internal [Bloxham, 2002, McFadden, 2007, Sarson, 2007].

42 A most direct research that relates geomagnetic variations and earthquakes is performed by the variations in the
43 ultra low frequency (ULF) in the magnetic field due the ionosphere-lithosphere-atmosphere coupling [Hayakawa et
44 al., 2015, De Santis, 2015, Contoyiannis et al., 2016, Potirakis et al., 2016, De Santis et al., 2017, Oikonomou et al.,
45 2017, Marchetti and Akhoondzadeh, 2018]. The spatial coupling at the earth's surface is given by $r = 10^{0.43M}$ (M:
46 earthquakes magnitude), and it means the maximum radius from the epicentre where evidence of magnetic
47 perturbations due ionosphere-lithosphere-atmosphere coupling is expected to be found [Dobrovolsky et al., 1979 ;
48 Pulinets and Boyarchuk, 2004, Oikonomou et al., 2017]. Table 2 shows that all magnetic measurements performed at
49 the stations of Putre and IPM are inside, or at the boundary of each radius determined by the earthquakes magnitude
50 of Maule, Iquique and Illapel, thus it is expected that the magnetic measurements are influenced by the ionosphere-
51 lithosphere-atmosphere coupling.

53 **3.0 Space Climate and the Seismic events of 27/2/2010 in Maule, 1/4/2014 in Iquique and 16/9/2015 in Illapel.**

55 The manifestation of space climate in the geomagnetic field during the periods concerned is defined by the Kp
56 magnetic activity index as shown in [Figure 1 a, b, c] for the months previous to the three earthquakes: Maule 2010
57 (Dec 12, 2009 to Mar 15, 2010), Iquique 2014 (Jan 1, 2014 to Apr 15, 2014) and Illapel 2015 (Jul 1, 2015 to Sep 30,
58 2015). For Maule 2010 the magnetic activity reached a kp index equal to or greater than 4 on only three isolated
59 occasions, it is therefore considered a calm period; for Iquique 2014, activity was concentrated around Feb 19, 2014
60 while for Illapel 2015 the maximum activity was recorded between Sep 8 and 10. In all three cases, activity did not
61 persist in time. The magnetic records for the B_z component show little external influence.

Annales
Geophysicae
Discussions

1   The magnetometer data in the OP and IPM stations for the Maule event run from Oct 31, 2009 to Apr 3, 2010; for
2   Iquique from Nov 15, 2013 to Apr 15, 2014 and for Illapel from Jul 1, 2015 to Sep 20, 2015. The Maule 2010 event had
3   a magnitude of Mw8.8 and occurred on Feb 27, 2010 at 06:34 UTC at a depth of 35 km, at 35.909°S, 72.733°W. Iquique
4   2014 had a magnitude of Mw8.2 and occurred on Apr 1, 2014 at 23:46 UTC at a depth of 25.0 km ± 1.8 km, at 19.610°S
5   70.769°W. Illapel 2015 had a magnitude of Mw8.3 and occurred on Sep 16, 2015 at 23:46 UTC at a depth of 22.4 km
6   ± 3.2 km [USGS].
7
8   Measurements of the B_z component [Figure 2] are represented by similar gradients in Iquique 2014 and Illapel 2015
9   to those found in Maule 2010, giving rise to a jump in each case. It is known that these magnetic signals are generated
10 by the earth's core and disseminated through the mantle, implying changes in its electrical conductivity [Stewart. et
11 al., 1995].
12
13 The jump in the B_z component for Maule 2010 was recorded in the OP station on Jan 23, 2010, a time lapse of 36 days
14 before the earthquake and the moment at which a change appears in the gradient or trend. It alters from a diminution
15 of 225 nT in the period Oct 31, 2009 to Jan 23, 2010, to a less abrupt diminution of 30 nT between Jan 23, 2010 and
16 Apr 3, 2010; prior to the jump on Jan 16, 2010 there is a small, abrupt diminution from -5048 nT to -4927 nT.
17 Discounting this small, abrupt diminution, the delta between the gradients falls from -4960 nT to -4926 nT, delta = 34
18 nT [Figure 2 a]. For Iquique 2014 the jump recorded in OP occurred on Dec 27, 2013, a time lapse of 96 days before
19 the earthquake. A change appears in the gradient on this date from a diminution of 123 nT in the period Nov 15, 2013
20 to Dec 27, 2013, to a diminution of 113 nT between Dec 27, 2013 and Apr 15, 2014; the jump presents a change from
21 -7355 nT to -7235 nT, delta = 120 nT [Figure 2 b]. For Iquique 2014 the jump measured at IPM occurred on Apr 3,
22 2014, a time lapse of 91 days before the earthquake. The trend shows a slight increase between Sep 30, 2013 and Jan
23 3, 2014, from -19116 nT to -19104 nT, while a further slight increase occurs in the period Jan 3, 2014 to May 6, 2014,
24 from -19101 nT to -19099 nT. The size of the jump was -3 nT [Figure 2 c]. For Illapel 2015 the jump measured at IPM
25 occurred on Aug 31, 2015, a time lapse of 16 days before the earthquake. The trend shows a slight diminution
26 between Aug 31, 2015 and Sep 20, 2015, from -19054 nT to -19072 nT, a jump of -11 nT.
27
28 Note that the gradient measured from Easter Island is the reverse of the gradients in the Maule and Iquique regions
29 [Figure 2 c]; the gradient is gentler because IPM is located on the opposite edge of the Nazca plate.
30
31 For the first derivative (secular variation of the B_z component) the maximum value (or peak value) observed for Maule
32 2010 was 141 nT/day on Jan 23, 2010. Two peaks are found for Iquique 2014, one of 84 nT/day on Dec 5, 2013 and
33 another one of 78 nT/day on Dec 28, 2013; one peak is recorded for Illapel 2015 of 8.0 nT/day. For the second
34 derivative (secular acceleration of the B_z component) a positive peak is recorded for Maule 2010 of 157 nT/day^2 on
35 Jan 22, 2010 and a negative peak of -116 nT/day^2 on Feb 24, 2010]. For Iquique 2014 a positive peak of 98 nT/day^2
36 was observed on Dec 29, 2013 and a negative peak of -127 nT/day^2 on Dec 31, 2013]. In Illapel 2015, during the days
37 immediately before the jump a negative peak of - 2 nT/day^2 was recorded on Aug 31, 2015 and a positive peak of 0.01
38 nT/day^2 on Sep 2, 2015. The frequency spectrum values were analysed for the Maule, Iquique and Illapel earthquakes.
39 Geophysical measurements are appropriate for highlighting fundamental frequencies; the frequencies generated in
40 these events ranged from 5.606 to 3.481 μ Hertz or from 1 cycle / 48.9 hours to 1 cycle / 79.13 hours.
41
42 In the Maule event, peaks for the frequencies 4.747; 5.064 and 5.154 μ Hertz were recorded [Figure 3 a]. In Iquique
43 peaks of 4.611; 4.882 and 5.154 μ Hertz were recorded [Figure 3 b]. And for Illapel 3.739; 4.630 and 5.520 μ Hertz
44 [Figure 3 c]. Before the Iquique 2014 event a jump in intensity was observed associated with the frequency of 5.154
45 μ Hertz [Figure 3 d] for the period Dec 27, 2013 to Jan 11, 2014, i.e. after the jump. Figure 3 e shows a jump in
46 intensity associated with the frequency of 3.739 μ Hertz during Sep 1, 2015 to Sep 8, 2015 before the Illapel 2015
47 event and subsequent to the jump. Figure 3 shows a jump in intensity associated with the frequency of 3.739 μ Hertz
48 during the period Sep 1, 2015 to Sep 8, 2015, prior to the Illapel 2015 event but after the jump.
49
50 Generalizing the analyses illustrated, we consider the spectrograms of the second derivate of the B_Z component (data
51 by minute) at the Easter Island station for the Maule 2010, Iquique 2014 and Illapel 2015 events [Figure 6a-b-
52 c][Rabiner and Schafer, 1978, Oppenheim et al., 1999]. In the Maule 2010 event, the spectrogram shows that the low
53 frequency behaviour around $\sim 0.01 - 0.3\ mHz$ appears to diminish slightly in magnitude after the event of Feb 27,
54 2010 [Figure 6a]. The spectrogram for Iquique 2014 is marked with two arrows, one corresponding to Jan 3 and the
55 other (right) to the day of the event (Apr 1) [Figure 4b]. Within this period the magnitude of the minimum frequency
56 oscillated between $0.01 - 0.5\ mHz$, however after the event the minimum frequencies tended to be around
57 $\sim 0.5\ mHz$, with occasional increases in frequencies close to $\sim 0.3\ mHz$. The spectrogram for Illapel 2015 is shown in
58 Figure 4c, which presents the time period with two arrows: Jul 24 on the left, and Sep 16 (date of the event) on the
59 right. It can be seen that the low frequencies in the period start to increase progressively, from $\sim 1.2\ mHz$ to
60 $\sim 0.01\ mHz$. After the event, the low frequency density appears to diminish, and the minimum frequency rises to
61 $\sim 1\ mHz$.
62
63

4. Daily cumulative numbers of anomalous behaviour in the component z of magnetic field over the surface of Earth for Maule 2010 Mw8.8, Iquique 2014 Mw8.2 and Illapel 2015 Mw8.3

In the method for cumulative magnetic anomaly in surface of earth, we used statistically an atypical or anomalous value, that is, data that it is quite far from the average values of the sample. So we compare real values of B_i with a more representative value of the sample, its average B_{ave}. We will call the difference between the two as the residual ΔB. Using the distribution of data we can define when a value is atypical or anomalous in a normal distribution by statistical definitions of Quartiles and Outliers. The data used in this section comes from the supermag network (http://supermag.jhuapl.edu/). The data has a sampling frequency of one data per minute, and a period of one year before and one year after each earthquake was chosen.

We create a filter that eliminates the frequencies averaged near Nyquist and establishes a filter that eliminates high frequencies. The option was to consider a moving average of five points weighted: $B_{ave} = aB_{i−2} + bB_{i−1} + cB_i + bB_{i+1} + aB_{i+2}$. In our case we use a = 0.07, b = 0.25 and c = 0.5 − 2a. The uncertainty of the Flux-gate magnetometers used in the OSO and PIL station is of $\delta B = ±0.1$ nT, which allows us to calculate the error propagation for averaged data $\delta B = \delta B_i + \delta B_{ave} = ±0.2$ nT, then the total uncertainty is $\Delta B_i + 0.2$ nT. The data considered are for periods Dst <10 nT, and only quiet magnetic data (6:00 - 05:00 Local time [Hitchmn et al., 1998]. 0.6745σ represents 50% of the data that is closer to the average. So that 50% of the data farther from the average should be added. Then we consider as anomaly δBa all the magnetic variations that are found at an amount $|\delta Ba|$ of the average value. If the threshold to define the far points is 50% plus the error, then the equation to define the threshold or anomalies is $|\Delta Ba| >= 0.6745\sigma + 0.2$ nT.

To analyse the earthquake of Maule, we used the stations of OSO (Chile). The data used are between the 16.00 to 05.00 local time and in periods of time with an index DST less than or equal to 10 nT. OSO is a station nearby to be approximately 450 km from the epicentre of the Earthquake Maule 2010. We use the ΔBa equation, applied to the z component of the OSO station. Its standard deviation obtained is 0.04020 nT (5 σ = 020104 nT), whereby the threshold is $|\Delta Ba| >= 0.22712$ nT. The total anomalies registered for the two years are of 229, a normalized version is shown in Figure 6. Between days Feb 27, 2009 and Jan 12, 2010 the anomalies register a linear behaviour. In the difference between anomalies and linear interpolation for the period shows an increase in the approximate anomaly amounts for three months (Apr 5, 2010). The Maule earthquake on Feb 2, 2010 (vertical red line), then starts another linear period for approximately 8 months (Nov 27, 2010) with a new increase in the number of anomalies until the end of the period, in this period there is a seismic swarm where some of these seismic movements are indicated with purple double arrow [Figure 6]. A version without the linear trend is shown in Figure 7a.

In the earthquake of Iquique, we used Pilar station in direction North-East of Cordova in Argentina to 1420 Km of epicentre (PIL). The data used are between the 16.00 to 05.00 local time and in periods of time with an index less than or equal to 10 nT. The PIL station has almost no data between Dec. 27, 2014 and Feb. 3, 2015, however, this lack of data will not affect further analysis as it is a relatively short period of time. It is also a period well after the Iquique earthquake (9 months). The Z component of the PIL station is shown in Figure 7b. It has the values σ = 0.05262 nT (5σ = 0.26310 nT), threshold $|0.23549|$ nT and a total of 165 anomalies. The interpolation takes place between Apr 1, 2013 and Oct 3, 2013. It presents three increases in the number of anomalies. The first on Oct 3, 2013, the second is on Jan 8, 2014 and the third is on Apr 1, 2014. The change on Jan 8, 2014 is the most noticeable change in trend.

In the Illapel earthquake there was a great activity in the space environment, as the DST for 2015 is less precise, we increased the requirement for the spatial filter. It was considered a DST less than or equal to 5 nT. The excess of anomalies related with space weather was eliminated for 5 days in the PIL station: they are Apr 2, 2015; Sep 24, 2015; Jan 31, 2016; May 16, 2016 and Aug 27, 2016. PIL is approximately 745 km from the epicentre, that is, a nearby station. The ΔB equation, applied to the z component, its standard deviation obtained is 0.04797 nT (5 σ = 026803 nT) where by the threshold is $|\Delta Ba| >= 0.23615$ nT). The total anomalies registered for the two years are of 71. Between days Sep 16, 2014 and May 3, 2015, the anomalies register a linear behaviour [Figure 7c]. There are two increases in the number of anomalies prior to the Illapel earthquake, the first on Apr 28, 2015 and the second as of Jul 18, 2015 being the most significant in the two years of records

The daily values of magnetic anomalies during a year before and one after the earthquake and the difference with the linear interpolation have been made for the North and East components of all the stations studied, which we do not include in this work, considering it redundancy.

Marchetti and Akhoondzadeh, (2018) referred to cumulative number of anomalous behaviour in the ionosphere, which we have rebuilding, modified and plotted, with our method [Figure 8]. The first anomalies seen near 130 days before the Mexico earthquake Mw8.2. They used in the study of cumulative numbers of anomalous track in ionosphere with indices |DST| < 20 nT. For detected rapidly variation of magnetic field on Y component used the method present in the Santis et al. (2017) (use of Cubic Splines instead of Moving Average.), and where indices that

1 is easily affected by lithospheric activity. In general using satellite night time electron density residual variation date,
2 in pre-defined allowed ranges, based in M how median and IQR with inter quartile range parameters. M = + 1.25 x
3 IQR.
4
5
6 **5. Discussion and Conclusions**
7 The most significant characteristics of the total magnetic field and its variations in the first and second derivatives are
8 found in the B_z component, which we observed and recorded in the Putre and IPM observatories. There is evidence
9 of a progressive increase in the phenomenon known as the South Atlantic Magnetic Anomaly (SAMA) Cordaro et al
10 (2019), generating greater deviation in the intensities present in the OP station [Figure 2 a] [Figure 2 b]. Combining
11 this information with data from the IPM station, the behaviour of the radial component of the geomagnetic field for
12 the three most significant seismic events in the Chilean Pacific sector during the period 2010-2015 was recorded and
13 it corroborates the magnetic relation with seismology shown by Potirakis et al. (2016), Contoyiannis et al. (2016) and
14 De Santis et al. (2017) using other methods. Furthermore, the same succession is observed in all the measurements
15 of this paper: Jump or second derivative of Bz, time lapse and seismic movement.
16
17 These jumps occur in different forms: in Putre they are significant, reaching values of tens of nT, while in IPM the
18 jump is barely 10nT. The time lapse between each jump and the seismic event differs in each event. For Maule 2010
19 it was 36 days, for Iquique 2014 it was 96 days, and for Illapel 16 days. This time difference may be due to an important
20 factor: it appears that the jump is not equally strong in the three events, since the jump before the Iquique 2014
21 event was considerably weaker than the one before Illapel 2015 [Figure 2], and preceded the event by a longer time
22 lapse (96 days). The more abrupt jump recorded in Illapel was followed by a shorter time lapse (16 days).
23
24 The secular variations are characterised by a peak on the day of the jump or the following day, while the secular
25 accelerations are characterised to a lesser degree by one positive and one negative peak. The frequency spectrum
26 found for each of the events in the second derivate of the geomagnetic field, or secular acceleration, demonstrate
27 the appearance of a range of frequencies between 3.5 and 5.5 μ Hertz [Figure 3 a, b and c]; there is a significant
28 increase in one or a group of frequencies specifically in the week of the jump [Figure 3 d, e]. This reflects the
29 oscillations of the radial magnetic field whose oscillation period takes from 2 to 4 days. We are therefore able to
30 propose a simple model for radial behaviour, associating a step function represented by the jump with a subsequent
31 oscillation represented by oscillations in a station in the field, e.g. Putre.
32
33 Figure 4 presents three spectrograms: All three show a reduction in the low frequency magnitude between $0.01 -$
34 $1\ mHz$ after the seismic events; the reductions for the Iquique and Illapel events are the most significant. Moreover,
35 for the Illapel 2015 event the spectrogram recorded a magnitude increase in the low frequency range $(0.01 - 1\ mHz)$
36 between Jul 24 and Sep 16; this increase was clearer than in the other events, possibly because the Illapel event
37 occurred at a similar latitude to the location of IPM (Illapel 2015: 31.573°S, IPM 27.171°S). The start of these increases
38 recorded in the spectrograms coincides with the dates identified as the jump in geomagnetic measurements for the
39 z component in the same station and in the frequency spectra obtained for the same time series [Figures 2 and 4].
40
41 Figure 5 shows the radial behaviour of the geomagnetic field at the Easter Island station for the Iquique 2014 event.
42 If this is compared with the records kept at the Putre station over the same period, we see that the gradients or trends
43 found in Putre and IPM are opposite; again, we see that the jump in IPM is of the order of 10 nT.
44
45
46 The records of the Putre station for the Illapel 2015 event [Figure 2c] show a change in the trend of the magnetic field
47 during the period from Sep 16 to Oct 8; this cannot be considered to be a time lapse, since the spectrogram (Figure
48 4c) shows no low frequency increase$(0.01 - 1\ mHz)$, there are only isolated increases lasting no more than one or
49 two days. The frequency range found for the second derivate of the radial component of the earth's magnetic field
50 $(0.01 - 1\ mHz)$ is within the typical range of the earth's free oscillations $(\sim 0.1 - 1\ mHz)$ or of tidal effects $(\sim 0.01 -$
51 $0.06\ mHz)$ [Casotto and Biscani, 2004, Park et al,. 2005], and is lower than De Santis et al. (2017) (~20mHz) due to
52 the fact that they use data from moving satellites and thus cannot cover lower frequency range. Furthermore, being
53 dependent on space weather, they must use few hours every night to record reliable data. Despite these technical
54 differences between satellites and ground level magnetometers used, the data show a time lapse between the start
55 of magnetic perturbations and earthquakes of order of one month (or even more) and it is similar to the time lapse
56 founded by De Santis et al. (2017).
57
58 In a complementary way, the magnetic anomalies method defined in section 4 was used. Figure 6 shows the daily
59 accumulated value of magnetic anomalies found for the vertical component at OSO station. The behavior of the
60 anomalies for the period of two years of data is relatively similar between the three events recorded at OSO and PIL
61 station (Figure 7). The three measurements show an initial stable period and a sudden increase in the number of daily
62 anomalies prior to the occurrence of the Maule, Iquique and Illapel earthquakes. Then a period appears again without
63 great variations. This described behavior is similar to that found by Marchetti and Akhoondzadeh (2018) for the

earthquake in Mexico using satellites (Figure 8). Figure 8 was carried out by applying a stricter spatial filter to that used by Marchetti and Akhoondzadeh (2018). This would indicate that the main source of anomalies could be in the lithosphere and not in outer space. It can be related to stress and electrification changes in rocks within the lithosphere (e.g. Tzanis and Vallianatos, 2002). However, the existence of a similar behavior in the anomalies recorded in the ionosphere suggests the existence of some coupling mechanism between the lithosphere, atmosphere and ionosphere.

We must repeat that we do not yet think that we can predict the future occurrence of these seismic events, since the seismological mechanism of seismic movements is not yet clear. However, a correlation does appear to exist between cumulative number of magnetic anomaly, jump, time lapse and seismic movement for Maule 2010, Iquique 2014 and Illapel 2015. This could be used as a tool to show the behaviour of some geophysical variables to indicate plate movements in the near but not immediate future. This condition, based on the increase of low frequencies($\mu Hz - mHz$), suggests that these magnetic variations in the radial component are probably a necessary but not sufficient condition on the Chilean margin; further investigation of this subject is required.

Acknowledgments

References:

Aki, K., (1979). Characterization of barriers on an earthquake fault. J. Geophys. Res. 84,6140–6148, 1979.

Balasis, G. and Mandea, M. (2007) Can electromagnetic disturbances related to the recent great earthquakes be detected by satellite magnetometers? Tectonophysics, 431, 173–195, 2007.

Bangs, N.L. and Cande, S.C. (1997). Episodic development of a convergent margin inferred from structures and process along the Southern Chile margin. Tectonics, 16, 489-503, 1997.

Bayanjargal, G. (2013). The Study of Westward Drift in the Main Geomagnetic Field. *International Journal of Geophysics*. Volume 2013, Article ID 202763, 12 pages http://dx.doi.org/10.1155/2013/202763, 2013.

Bloxham, J., Zatman, S. and Dumberry, M. (2002). The origin of geomagnetic jerks. *Nature* 420, 65-68 (7 November 2002). doi:10.1038/nature01134, 2002.

Buffett, B. (2014). Geomagnetic fluctuations reveal stable stratification at the top of the Earth's core. 484-487 *Nature* Vol 507 27 March 2014 doi:10.1038/nature13122, 2014.

Calkins, M.A., Noir,J., Eldredge, J.D. and Aurnou, J.M. (2012). The effects of boundary topography on convection in Earth's core. Geophys. J. Int. (2012) 189, 799–814. doi: 10.1111/j.1365-246X.2012.05415.x, 2012.

Casotto, S. and Biscani, F. (2004). "A fully analytical approach to the harmonic development of the tide-generating potential accounting for precession, nutation, and perturbations due to figure and planetary terms", AAS Division on Dynamical Astronomy, April 2004, vol. 36(2), 67, 2004.

Chulliat, A., Lalanne, X., Gaya-Pique, L.R., Truong, F. and Savary, J. (2009). The new Easter Island magnetic observatory, in Proceedings of the XIIIth IAGA Workshop on Geomagnetic Observatory Instruments, Data Acquisition and Processing, edited by J. J. Love, 271 pp., U.S. Geological Survey Open-File Report 2009-1226, 2009.

Contoyiannis, Y., Potirakis, S.M., Eftaxias, K., Hayakawa, M., Schekotov, A., (2016). Intermittent criticality revealed in ULF magnetic fields prior to the 11 March 2011 Tohoku earthquake (Mw = 9). Physica A 452, 19–28. http://dx.doi.org/10.1016/j.physa.2016.01.065, 2016.

Contreras-Reyes E. and Carrizo, D. (2011). Control of high oceanic features and subduction channel on earthquake ruptures along the Chile–Peru subduction zone. Physics of the Earth and Planetary Interiors 186 (2011) 49–58, 2011.

Cordaro, E.G., Olivares, E., Gálvez, D., Salazar-Aravena, D., Laroze, D., (2012). New 3He neutron monitor for Chilean osmic-ray observatories from the Altiplanic Zone to the Antarctic zone. Adv. Space Res. 49, 1670, 2012.

Annales
Geophysicae
Discussions

Open Access

EGU

1
2 Cordaro, E.G., D. Gálvez, D. Laroze (2016). Observation of intensity of cosmic rays and daily magnetic shifts near meridian 70° in the
3 South America. *Journal of Atmospheric and Solar-Terrestrial Physics.* Volume 142, May 2016, Pages 72–82.
4 doi:10.1016/j.jastp.2016.02.015, 2016.
5
6 Cordaro, E.G., Venegas, P. and Laroze, D. (2018), Latitudinal variation Rate of Geomagnetic Cutoff Rigidity in the active Chilean
7 convergent margin. *Annales Geophysicae Angeo-2017-176.* 2018 .doi: 10.5194/angeo-36-275-2018, 2018.
8
9 Cordaro, E.G., Venegas-Aravena, P. and Laroze, D. (2019), Variation of geomagnetic cutoff rigidity in the sourthern hemisphere close
10 to 70°W (South-Atlantic Anomaly and Antarctic zones) in the period 1975-2010, Advances in Space Research,
11 https://doi.org/10.1016/j.asr 2018.12. 019.
12
13 Courtillot V., Ducruix, J., Le Mouël, J.-L. (1978). Sur une accélération récente de la variation séculaire du champ magnétique terrestre.
14 C.R. Acad. Sci. D 287 (1978) 1095-1098, 1978.
15
16 Cox G.A., Livermore, P.W. and Mound, J.E. (2016). The observational signature of modelled torsional waves and comparison to
17 geomagnetic jerks, *Physics of the Earth and Planetary Interiors* 255 (2016) 50–65 doi:10.1016/j.pepi.2016.03.012, 2016.
18
19 Das, S. and Aki, K. (1977). Fault plane with barriers: a versatile earthquake model. J. Geophys. Res. 82, 5658–5670, 1977.
20
21 Delouis, B., Nocquet, J.-M. and Vallée, M. (2010). Slip distribution of the February 27, 2010 Mw = 8.8 Maule Earthquake, central
22 Chile, from static and high-rate GPS, InSAR, and broadband teleseismic data, Geophys. Res. Lett., 37, L17305,
23 doi:10.1029/2010GL043899, 2010.
24
25 De Santis A., De Franceschi, G., Spogli, L., Perrone, L., Alfonsi, L., Qamili, E., Cianchini, G., Di Giovambattista, R., Salvi, S., Filippi, E.,
26 Pavón-Carrasco, F.J., Monna, S., Piscini, A., Battiston, R., Vitale, V., Picozza, P.G., Conti, L., Parrot, M., Pinçon, J.-L., Balasis, G., Tavani,
27 M., Argan, A., Piano, G., Rainone, M.L., Liu, W. and Tao, D. (2015). Geospace perturbations induced by the Earth: The state of the
28 art and future trends. Physics and Chemistry of the Earth 85–86 (2015) 17–33. http://dx.doi.org/10.1016/j.pce.2015.05.004, 2015.
29
30 De Santis A., Balasis G., Pavón-Carrasco, F.J. Cianchini G. and Mandea M. (2017). Potential earthquake precursory pattern from
31 space: The 2015 Nepal event as seen by magnetic Swarm satellites. Earth and Planetary Science Letters 461 (2017) 119–126.
32 http://dx.doi.org/10.1016/j.epsl.2016.12.037, 2017.
33
34 Diaz-Naveas, J.L. (1999). Sediment subduction and accretion at the Chilean convergent margin between 35∘ und 40∘S, PhD thesis.
35 Ch.-A.-Univ., Kiel, Germany, 1999.
36
37 Dobrovolsky, I.R., Zubkov, S.I. and Myachkin, V.I. (1979). Estimation of the size of earthquake preparation zones. Pure Appl. Geophys.
38 117, 1025–1044, 1979.
39
40 Farías M., Comte, D., Roecker, D., Carrizo, D. and Pardo, M. (2011). Crustal extensional faulting triggered by the 2010 Chilean
41 earthquake: The Pichilemu Seismic Sequence. TECTONICS, VOL. 30, TC6010, doi: 10.1029/2011TC002888, 2011.
42
43 Finlay, C. (2007). *Magnetohydrodynamics Waves*, Encyclopedia of Geomagnetism and Paleomagnetism, Edited by D. Gubbins and
44 E. Herrero-Berbera. Springer, Netherlands, 2007.
45
46 Fisher, R.A. (1958) Statistical Methods for Research Workers, 13th Ed., Hafner, 1958.
47
48 Florindo, F., Alfonsi, L., Piersanti, A., Spada, G. and W. Marzocchi (1996). Geomagnetic jerks´ and seismic activity. Annali di Geofisica,
49 39, 1227-1233, 1996.
50
51 Gjerloev, J. W. (2012). The SuperMAG data processing technique, *J. Geophys. Res.*, 117 A09213, doi: 10.1029/2012JA017683, 2012.

52 Hartmann, G. A., and Pacca, I. G. (2009). Time evolution of the South Atlantic Magnetic Anomaly. Ann. Braz. Acad. Sci. 81, 243–255.
53 doi: 10.1590/S0001-37652009000200010, 2009.

54 Hayakawa, M. and Molchanov, O.A. (eds.) (2002). Seismo Electromagnetics: Lithosphere-Atmosphere-Ionosphere Coupling.
55 TERRAPUB, Tokyo, 2002.

56 Hayakawa, M., Schekotov, A., Potirakis, S., Eftaxias, K. (2015). Criticality features in ULF magnetic fields prior to the 2011 Tohoku
57 earthquake. Proc. Jpn. Acad. Ser. B, Phys. Biol. Sci. 91, 25–30. http://dx.doi.org/10.2183/pjab.91.25, 2015.

58 He, G., Wong, T.-f. and Beeler, N. M. (2003). Scaling of stress drop with recurrence interval and loading velocity for laboratory-
59 derived fault strength relations Journal of Geophysical research, Vol. 108, N° B1, 2037, doi:10.1029/2002JB001890, 2003.

60 Heirtzler, J. R. (2002). The future of the South Atlantic anomaly and implications for radiation damage in space. J. Atmos. Solar Terr.
61 Phys. 64, 1701–1708. doi: 10.1016/s1364-6826(02)00120-7, 2002.

62 Hitchmn, A.P, Lilley, F.E.M. and Campbell, W.H. (1998). The quiet daily variation in the total magnetic field: global curves.
63 GEOPHYSICAL RESEARCH LETTERS, VOL. 25, NO. 11, PAGES 2007-2010, JUNE 1, 1998.

1   Jackson, A., Jonkers, A.R.T. and Walker, M.R., (2000). Four centuries of geomagnetic secular variation from historical records, Phil.
2   Trans. R. Soc. A, 358, 957–990, 2000.

3   Jault, D. (2003), Electromagnetic and topographic coupling, and LOD variations. In: Jones CA, Soward AM, and Zhang K (eds.) *Earth's*
4   *Core and Lower Mantle* (2003), pp. 55–76. Boca Raton, FL: CRC Press, 2003.
5
6   Jault, D. and Finlay, C.C. (2015). Waves in the Core and Mechanical Core–Mantle Interactions, Treatise on Geophysics (Second
7   Edition) 2015, Pages 225–244. Reference Module in Earth Systems and Environmental Sciences Volume 8: Core Dynamics,
8   doi:10.1016/B978-0-444-53802-4.00150-0, 2015.

9   Jeanloz, R. and Romanowic, B. (1997). Geophysical Dynamics at the Center of the Earth. *Physics Today*. 50 (1997) 22 – 27, 1997.
10
11 Kanamori, H. (1994). Mechanics of earthquakes. Annu. Rev. Earth Planet. Sci. 22,207–237, 1994.
12
13 Kendall, M.G. (1979). The Advanced Theory of Statistics, 4th Ed., Macmillan, 1979.
14
15 Koelemeijer, P.J., Deuss, A., and Trampert, J. (2012). Normal mode sensitivity to Earth's D'' layer and topography on the core–mantle
16 boundary: What we can and cannot see. Geophysical Journal International 190: 553–568, 2012.
17
18 Koper, K.D., Pyle, M.L., and Franks, J.M. (2003). Constraints on aspherical core structure from PKiKP-PcP differential travel times.
19 Journal of Geophysical Research 108: 2168. http://dx.doi.org/10.1029/2002JB001995, 2003.
20
21 Lassak, T., McNamara, A., Garnero, E., and Zhong, S. (2010). Core–mantle boundary topography as a possible constraint on lower
22 mantle chemistry and dynamics. *Earth and Planetary Science Letters* (2010) 289: 232–241, 2010.
23
24 Le Huy, M., Alexandrescu, M., Hulot, G. and Le Mouël, J.-L. (1998). On the characteristics of successive geomagnetic jerks. Earth.
25 *Earth Planets Space*, 50, 723–732, 1998.
26
27 Liu, J.Y. (2009). Earthquake precursors observed in the ionospheric F-region. In Electromagnetic Phenomena Associated with
28 Earthquakes (ed. Hayakawa, M.). Transworld Research Network, Trivandrum, India, pp. 187–204, 2009.
29
30 Lorito, S., Romano, F., Atzori, S., Tong, X., Avallone, A., McCloskey, J., Cocco, M., Boschi, E. and Piatanesi, A. (2011). Limited overlap
31 between the seismic gap and coseismic slip of the great 2010 Chile earthquake, Nat. Geosci., 4, 173–177, doi:10.1038/ngeo1073,
32 2011.
33
34 Love, J.J. and Thomas, J.N. (2013). Insignificant solar-terrestrial triggering of earthquakes. GEOPHYSICAL RESEARCH LETTERS, VOL.
35 40, 1165–1170, doi:10.1002/grl.50211, 2013.
36
37 Malin, S.R.C., Hodder, B.M. and Barraclough, D.R. (1983). Geomagnetic secular variation: A jerk in 1970. In Observatorio del Ebro
38 Sci. Contrib. in Commemoration of Ebro Observatory's 75th Anniv. Roquetes, Tarragona, 1983. p 239-256 (SEE N85-13308 04-42),
39 1983.
40
41 Mandea, M., Bellanger, E. and Le Mouël, J.-L. (2000). A geomagnetic jerk for the end of the 20th century? Earth and Planetary Science
42 Letters 183 (2000) 369-373, 2000.
43
44 Marchetti, D and Akhoondzadeh, M. (2018). Analysis of Swarm satellites data showing seismo-ionospheric anomalies around the
45 time of the strong Mexico (Mw = 8.2) earthquake of 08 September 2017. Advances in Space Research 62 (2018) 614–623,
46 https://doi.org/10.1016/j.asr.2018.04.043, 2018.
47
48 McFadden, P.L. and Merrill, R.T. (2007). *Geomagnetic Field, Asymmetries*, Encyclopedia of Geomagnetism and Paleomagnetism,
49 Edited by D. Gubbins and E. Herrero-Berbera. Springer, Netherlands, 2007.
50
51 Molchanov, O.A. and Hayakawa, M. (2008). SeismoElectromagnetics and Related Phenomena: History and Latest Results.
52 TERRAPUB, Tokyo, 2008.
53
54 Oikonomou, C., Haralambous, H. and Muslim, B. (2017). Investigation of ionospheric precursors related to deep and intermediate
55 earthquakes based on spectral and statistical analysis. Advances in Space Research 59 (2017) 587–602.
56 http://dx.doi.org/10.1016/j.asr.2016.10.026, 2017.
57
58 Olsen, N., Luehr, H., Sabaka, T.J., Michaelis, I., Rauberg, J. and TøffnerClausen, L. (2014). The CHAOS-4 geomagnetic field model,
59 Geophys. J. Int., 197, 815–827, 2014.
60
61 Olson, P., Christensen, U.R. and Glatzmaier, G.A. (1999). Numerical modeling of the geodynamo: mechanisms of field generation
62 and equilibration, J. geophys. Res., 104, 10 383–10 404, 1999.
63
64 Olson, P. (2015). Core Dynamics: An Introduction and Overview, Treatise on Geophysics (Second Edition) 2015, Pages 1–25
65 Reference Module in Earth Systems and Environmental Sciences Volume 8: Core Dynamics doi:10.1016/B978-0-444-53802-4.00137-
66 8, 2015.
67
68 Oppenheim, A.V., Schafer, R.W., and Buck, J. R. (1999). Discrete-Time Signal Processing. 2nd Ed. Upper Saddle River, NJ: Prentice
69 Hall, 1999.

Park, J., Song, T.-R. A., Tromp, J., Okal, E., Stein, S., Roult, G., Clevede, E., Laske, G., Kanamori, H., Davis, P., Berger, J., Braitenberg, C., Van Camp, M., Lei, X., Sun, H., Xu, H. and Rosat, S. (2005). Earth's Free Oscillations Excited by the 26 December 2004 Sumatra-Andaman Earthquake. Science 20 May 2005: Vol. 308, Issue 5725, pp. 1139-1144. DOI: 10.1126/science.1112305, 2005.

Plotkin, V.V. (2016). Jerks and conductivity anisotropy of lower mantle, *Russian Geology and Geophysics* Volume 57, Issue 2, February 2016, Pages 344-355 doi:10.1016/j.rgg.2016.02.011, 2016.

Pomerantz, M.A. (1971). Cosmic Rays. Published by The Commission on College Physics. Rd. Van Nostrand Reinhold Company, 1971.

Potirakis, S., Eftaxias, K., Schekotov, A., Yamaguchi, H. and Hayakawa, M., (2016). Criticality features in ultra-low frequency magnetic fields prior to the 2013 M6.3 Kobe earthquake. Ann. Geophys. 59 (3), S0317. http://dx.doi.org/10.4401/ag-6863, 2016.

Potirakis, S.M., Asano, T. and Hayakawa, M., (2018). Criticality Analysis of the Lower Ionosphere Perturbations Prior to the 2016 Kumamoto (Japan) Earthquakes as Based on VLF Electromagnetic Wave Propagation Data Observed at Multiple Stations. Entropy 2018, 20, 199; doi: 10.3390/e20030199, 2018.

Press, W.H., Teukolsky, S.A., Vetterling, W.T., and Flannery, B.P (1992). Numerical Recipes in C, 2nd Ed., Cambridge University Press, 1992.

Pulinets, S. and Boyarchuk, K. (2004). Ionospheric Precursors of Earthquakes. Springer, Berlin, 2004.

Rabiner, L.R. and Schafer, R.W. (1978). Digital Processing of Speech Signals. Englewood Cliffs, NJ: Prentice-Hall, 1978.

Ranero, C.R., von Huene, R., Weinrebe, W. and Reichert, C., (2006). Tectonic processes along the Chile convergent margin, in The Andes-Active Subduction Orogeny, Frontiers in Earth Sciences, pp. 91–121, eds Oncken, O. et al., Springer, Berlin, 2006.

Ranjith, K., and Rice, J.R. (1999). Stability of quasi-static slip in a single degree of freedom elastic system with rate and state dependent friction, J. Mech. Phys. Solids, 47, 1207 – 1218, 1999.

Sarson, G.R. (2007). *Dynamo Waves*, Encyclopedia of Geomagnetism and Paleomagnetism, Edited by D. Gubbins and E. Herrero-Berbera. Springer, Netherlands, 2007.

Scherwath, M., Contreras-Reyes, E., Flueh, E.R., Grevemeyer, I., Krabbenhoeft, A., Papenberg, C., Petersen C.J. and Weinrebe, R.W. (2009). Deep lithospheric structures along the southern central Chile margin from wide-angle P-wave modelling. Geophys. J. Int. (2009) 179, 579–600. doi: 10.1111/j.1365-246X.2009.04298.x, 2009.

Scoville, J., Heraud, J. and Freund, F. (2015). Pre-earthquake magnetic pulses. Nat. Hazards Earth Syst. Sci., 15, 1873–1880, 2015. doi:10.5194/nhess-15-1873-2015, 2015.

Shea, M.A. and Smart, D.F. (2001). Vertical cutoff rigidities for cosmic ray stations since 1955. Proceedings of the 27th International Cosmic Ray Conference. 07-15 August, 2001. Hamburg, Germany. p.4063, 2001.

Simmons, N.A., Forte, A.M., Boschi, L. and Grand, S.P. (2010). Gypsum: A joint tomographic model of mantle density and seismic wave speeds. *Journal of Geophysical Research* (2010) 115: B12310. http://dx.doi.org/10.1029/2010JB007631, 2010.

Smart, D.F. and Shea, M.A. (2004). A review of geomagnetic cutoff rigidities for earth-orbiting spacecraft. *Advances in Space Research* 36 (2005) 2012–2020. doi:10.1016/j.asr.2004.09.015, 2004.

Soldati, G., Boschi, L., and Forte, A.M. (2010). Tomography of core–mantle boundary and lowermost mantle coupled by geodynamics. *Geophysical Journal International* (2012) 189: 730–746, 2010.

Soloviev, A., Chulliat, A., Bogoutdinov, S., Gvishiani, A., Agayan, S., Peltier, A. and Heumez, B. (2012). Automated recognition of spikes in 1 Hz data recorded at the Easter Island magnetic observatory. Earth Planets Space, 64, 743–752, 2012.

Space Physics Interactive Data Resource Home - *NOAA*: http://spidr.ngdc.noaa.gov/spidr/

Stewart, D.N., Busse, F.H., Whaler, K. and Gubbins, D. (1995). Geomagnetism Earth rotation and the electrical conductivity of the lower mantle. Phys. Earth Planet. Inter., 92, 199-214), 1995.

Storini, M., Shea, M.A., Smart, D.F. and Cordaro, E.G. (1999). Cutoff Variability for the Antarctic Laboratory for Cosmic Rays (LARC: 1955-1995) 26th International Cosmic Ray Conference. SH.3.6.30 .7 1999. 402], 1999.

Terra-Nova, F., Amit, H., Hartmann, G.A. and Trindade. R.I.F. (2016). Using archaeomagnetic field models to constrain the physics of the core: robustness and preferred locations of reversed flux patches. Geophys. J. Int. (2016) 206, 1890–1913 doi: 10.1093/gji/ggw248, 2016.

Thomas, J.N., Love, J.J., Komjathy, A., Verkhoglyadova, O.P., Butala, M. and Rivera, N. (2012). On the reported ionospheric precursor of the 1999 Hector Mine, California earthquake, Geophys. Res. Lett., 39, L06302, doi:10.1029/2012GL051022, 2012.

Annales
Geophysicae
Discussions

Open Access

EGU

1   Thomas, J.N., Love, J.J. and Johnston M.J.S. (2009a). On the reported magnetic precursor of the 1989 Loma Prieta earthquake.
2   Physics of the Earth and Planetary Interiors 173 (2009) 207–215. doi:10.1016/j.pepi.2008.11.014, 2009a.
3
4   Thomas, J.N., Love, J.J., Johnston, M.J.S., and Yumoto, K. (2009b). On the reported magnetic precursor of the 1993 Guam earthquake,
5   Geophys. Res. Lett., 36, L16301, doi:10.1029/2009GL039020, 2009b.
6
7   Tzanis, A. and Vallianatos, F. (2002). A physical model of electrical earthquake precursors due to crack propagation and the motion
8   of charged edge dislocations, in: Seismo Electromagnetics (Lithosphere–Atmosphere–Ionosphere-Coupling), TerraPub, 2002, pp.
9   117–130, 2002.
10
11 Tzanis, A. (2010). An examination of the possibility of earthquake triggering by the ionosphere–lithosphere electro-mechanical
12 coupling. Hellenic Journal of Geosciences, vol.45, 307-316, 2010.
13
14 U.S. Geological Survey, Earthquake Hazards Program: http://earthquake.usgs.gov/earthquakes/
15
16 Vallianatos, F. and Tzanis, A. (2003). On the nature, scaling and spectral properties of pre-seismic ULF signals. Natural Hazards and
17 Earth System Sciences (2003) 3: 237–242. European Geosciences Union, 2003.
18
19 Varotsos, P.A. (2005). The Physics of Seismic Electric Signals. TERRAPUB, Tokyo, 2005.
20
21 Vestine, E.H. (1953). On variations of the geomagnetic field, fluid motions, and the rate of the earth's rotation. J. Geophys. Res., 58,
22 127-145, 1953.
23
24 Vezzoli, L. and Acoocella, V. (2009). Easter Island, SE Pacific: An end-member type of hotspot volcanism. Geological Society of
25 American Bulletin, May/june 2009, V. 121; no 5/6, p 869-886, doi:10.1130/B26470.1, 2009.
26
27 Villalobos, C.U., Bravo, M.A., Ovalle, E.M. and Foppiano, A.J. (2016). Ionospheric characteristics prior to the greatest earthquake in
28 recorded history. Advances in Space Research, 57 (2016) 1345–1359. http://dx.doi.org/10.1016/j.asr.2015.09.015, 2016.
29
30 World Data Center for Geomagnetism, Kyoto. *Data Analysis Center for Geomagnetism and Space Magnetism.*
31 *Graduate School of Science, Kyoto University.* Kitashirakawa-Oiwake Cho, Sakyo-ku, Kyoto 606-8502, JAPAN http://wdc.kugi.kyoto-
32 u.ac.jp/.
33
34 Yoshida, M. (2008). Core–mantle boundary topography estimated from numerical simulations of instantaneous mantle flow.
    Geochemistry, Geophysics, Geosystems 9 (2008): Q07002. http://dx.doi.org/10.1029/2008GC002008, 2008.

35
36
37
38
39
40
41
42
43
44
45
46
47
48
49
50
51
52
53
54
55
56
57
58
59
60
61
62
63
64

1
2
3
4
5
6
7   **Captions**
8
9
10   Figure 1: The Kp magnetic activity index for the periods prior to the Maule 2010 (top), Iquique 2014 (middle) and Illapel 2015
11   (bottom) earthquakes. [spidr NOAA] [WDCFG Kyoto University]
12
13   Figure 2: Component B_z at the Putre station for a) Maule 2010 and b) Iquique 2014; c) Easter Island station for Illapel 2015
14
15   Figure 3: Fourier Fast Transform (FFT) of the B''_z component in the Putre station for a) Maule 2010 and b) Iquique 2014; c) Easter
16   Island for Illapel 2015; d) FT every 16 days for Iquique 2015 from the Putre magnetometer; e) FFT every 8 days for Illapel 2015 from
17   the Easter Island magnetometer
18
19   Figure 4: Spectrograms with the behaviour of frequencies around 0.5 mHz, in periods close to the Maule 2010, Iquique 2014 and
20   Illapel 2015 seismic events
21
22   Figure 5: Trend for the Bz component to increase at Easter Island station after the jump on Dec 27, 2013 prior to the Iquique 2014
23   event.

24   Figure 6: The difference between anomalies and lineal interpolation in the period, for OSO Station in Maule event

25   Figure 7a, b, c: Accumulated Diary of magnetic anomalies during two years, in component Z, for Maule, Iquique and Illapel Events

26   Figure 8: Figure rebuild, modified, normalized and adapted with our method from Marchetti and Akhoondzadeh (2018). Upper
27   panel: Accumulated Diary of magnetic anomalies during two years, in component Y from Apr 1 to Oct 15, 2017 in Mexico Earthquake
28   Sep 8, 2017 Mw8.2 and Lower panel: Residual behaviour of Mexico Earthquake.

29

30   Tables

31
32   Table 1. The main characteristics for the detector of Chilean network Cosmic Rays and Geomagnetic Observatories as location,
33   altitude, and atmospheric deept, type of detectors.
34
35   Table 2. The maximum radius where the ionosphere-lithosphere-atmosphere coupling may affect magnetic measurements to each
36   earthquake studied at the station of Putre and IPM [Dobrovolsky et al., 1979 ; Pulinets and Boyarchuk, 2004].

37

Annales
Geophysicae
Discussions

Open Access

EGU
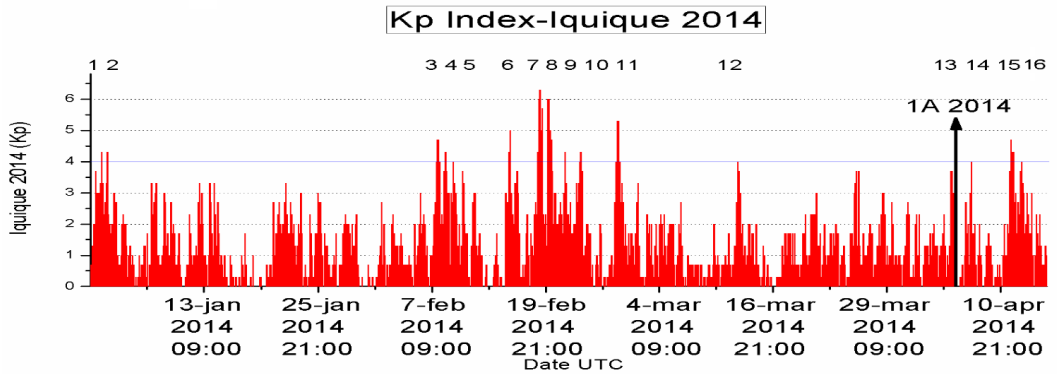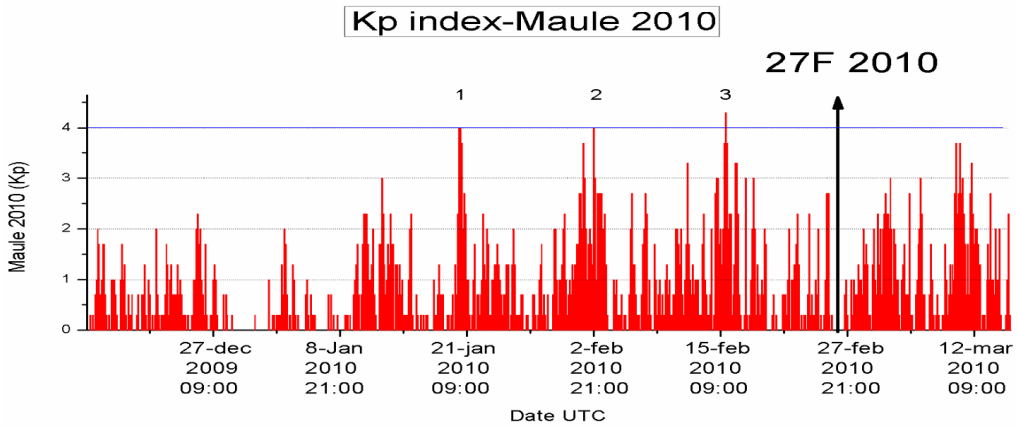
1   Figure 1
2
3
4
5
6

7
8

9
10
11
12

1   Figura 2

Bz Iquique 2014 / Putre Station

2
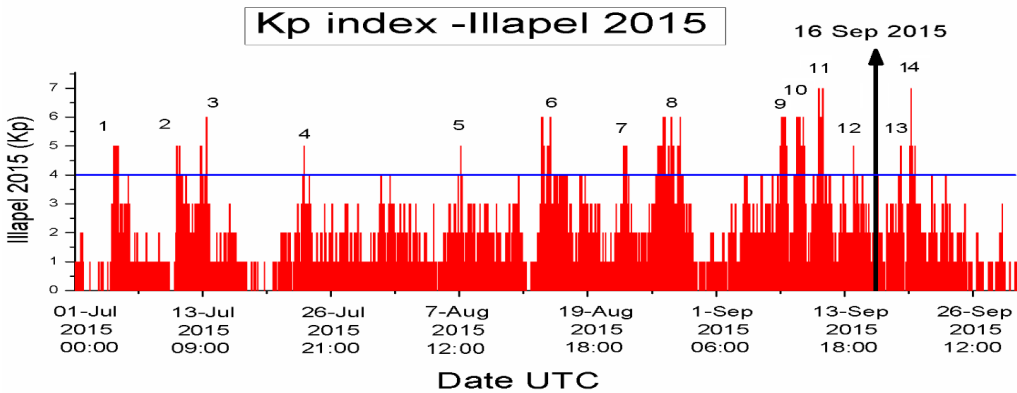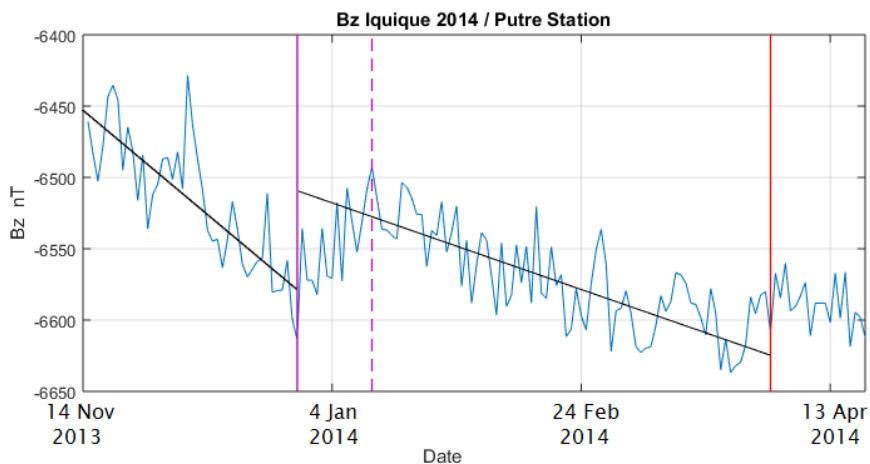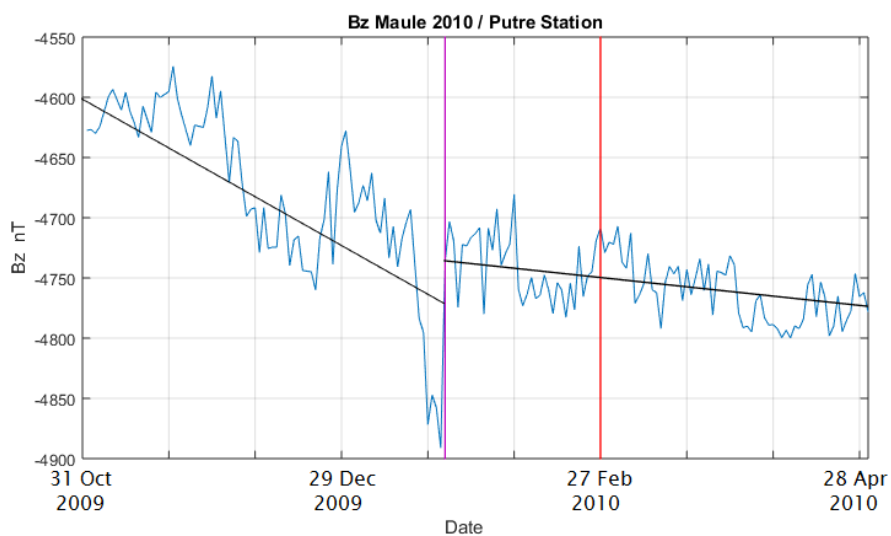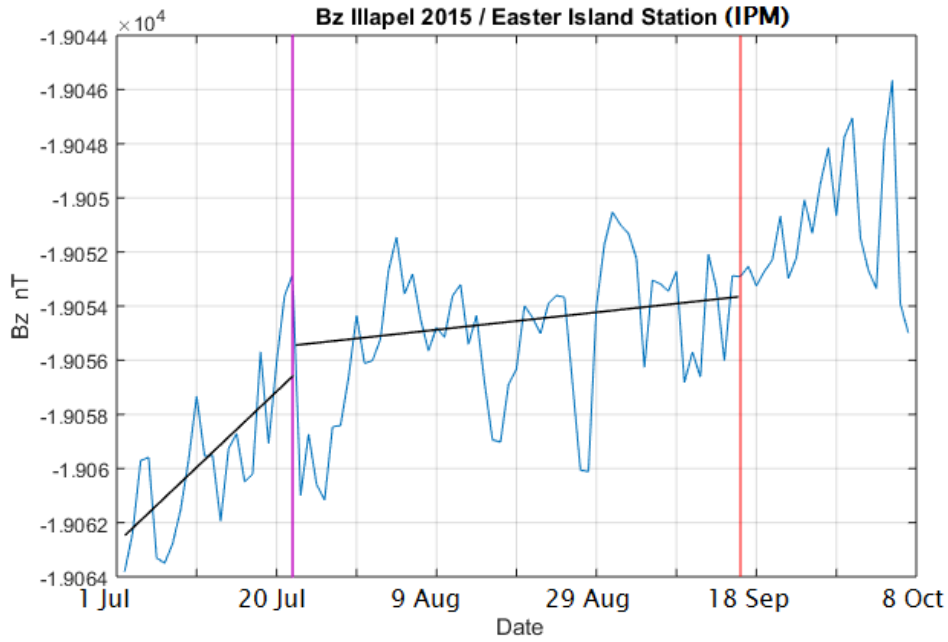
Bz Maule 2010 / Putre Station

3
4
5
6
7
8
9
10
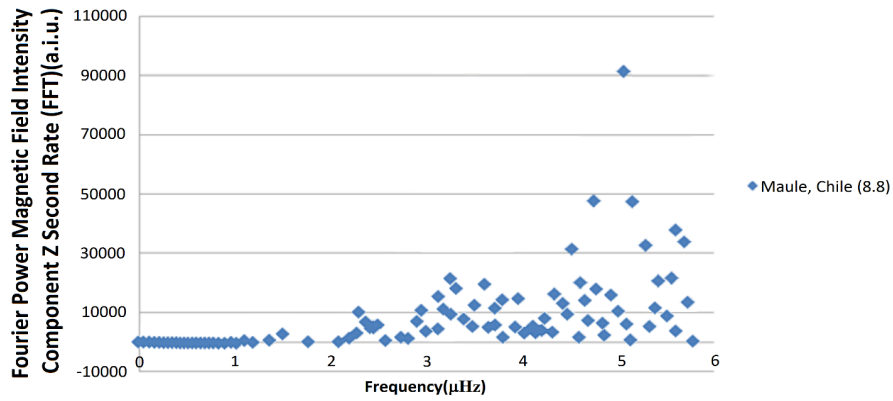
Figura 3

Bz'' FFT Iquique 2014 / Putre Station
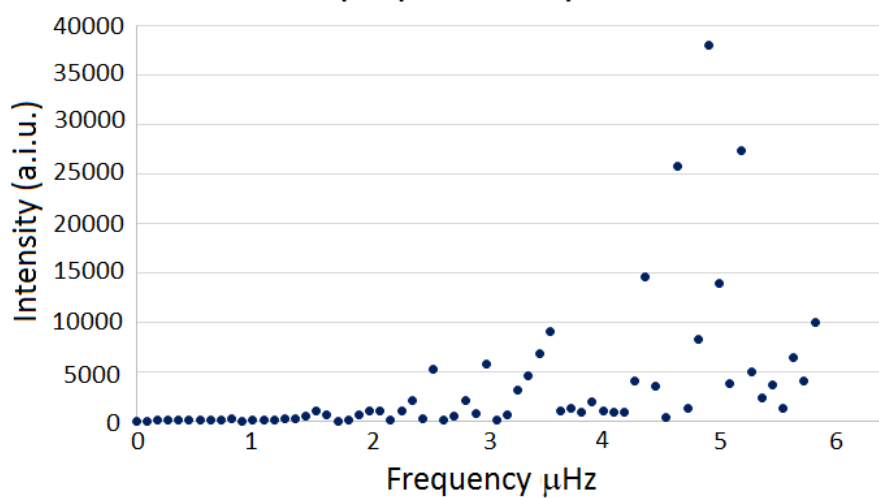
1
2
3

Bz'' FFT Illapel 2015 / Easter Island Station

4
5
6

Annales
Geophysicae
Discussions

Open Access

EGU
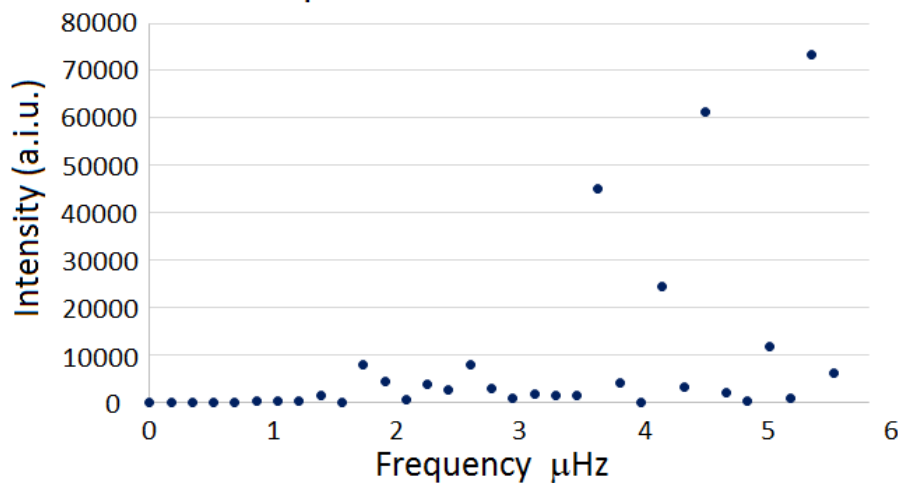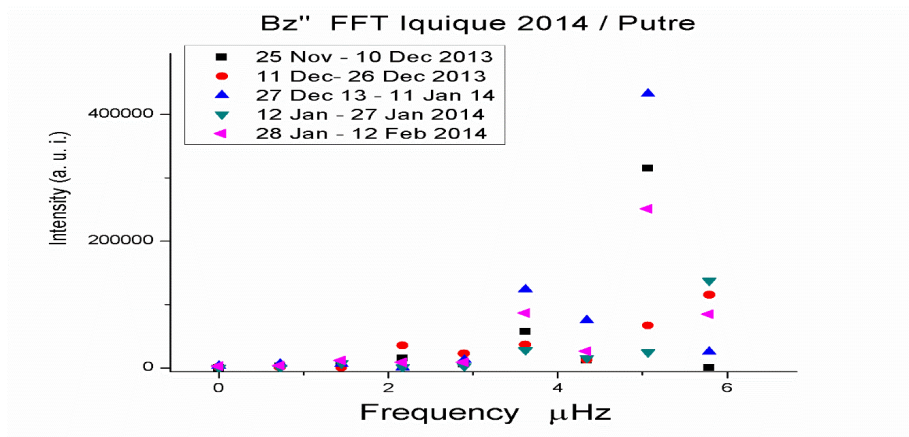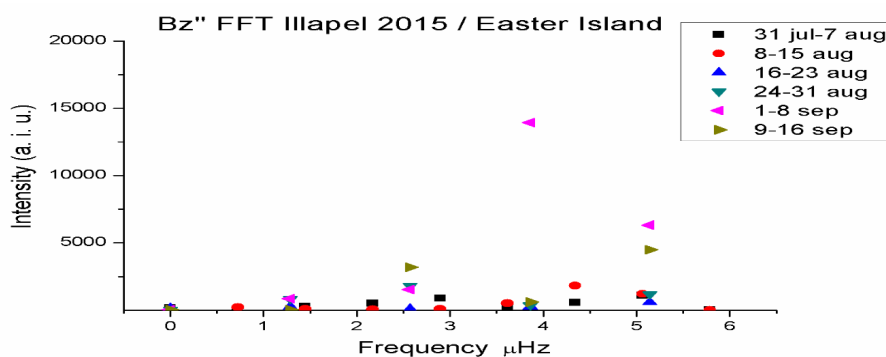
1
2
3
4
5
6
7
8
9
10
11
12
13
14
15
16
17
18
19
20

1   Figura 4
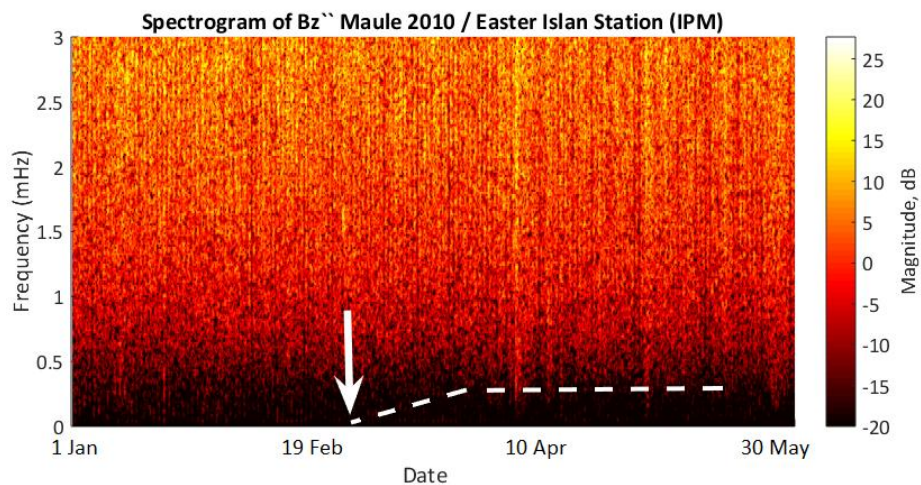
2
3
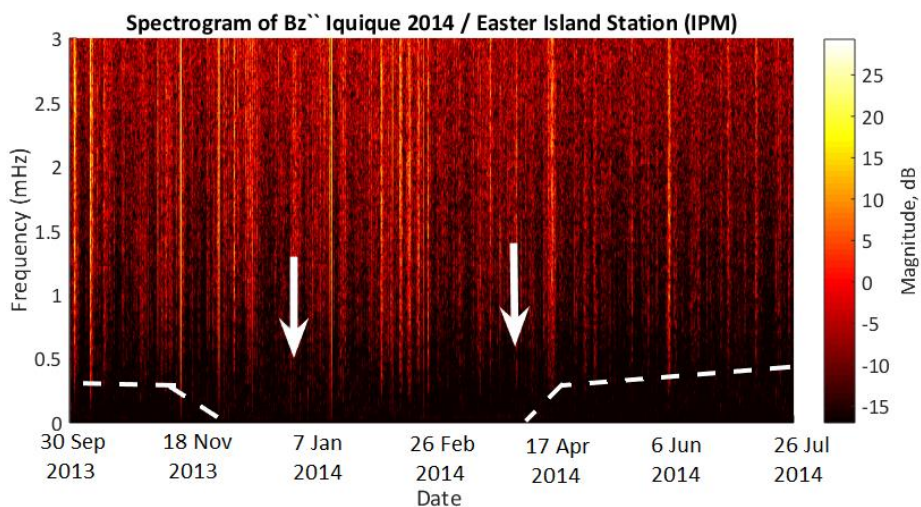
4
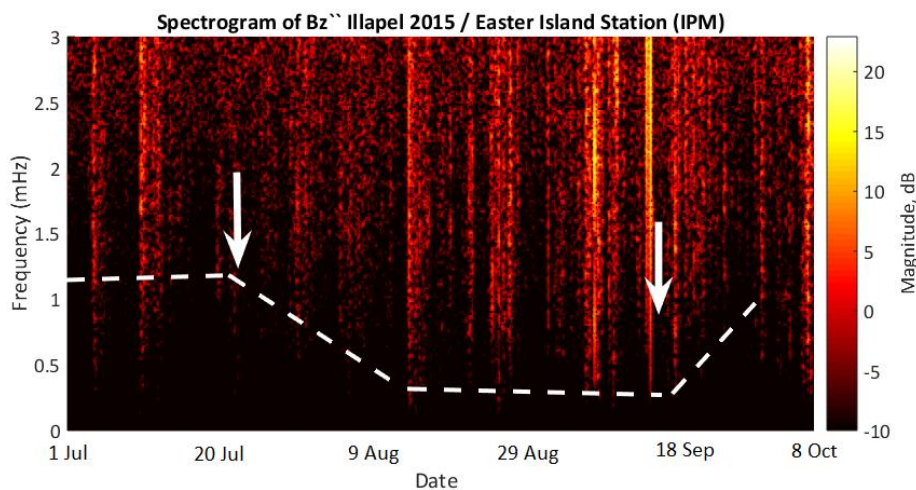
1

2

3   Figura 5
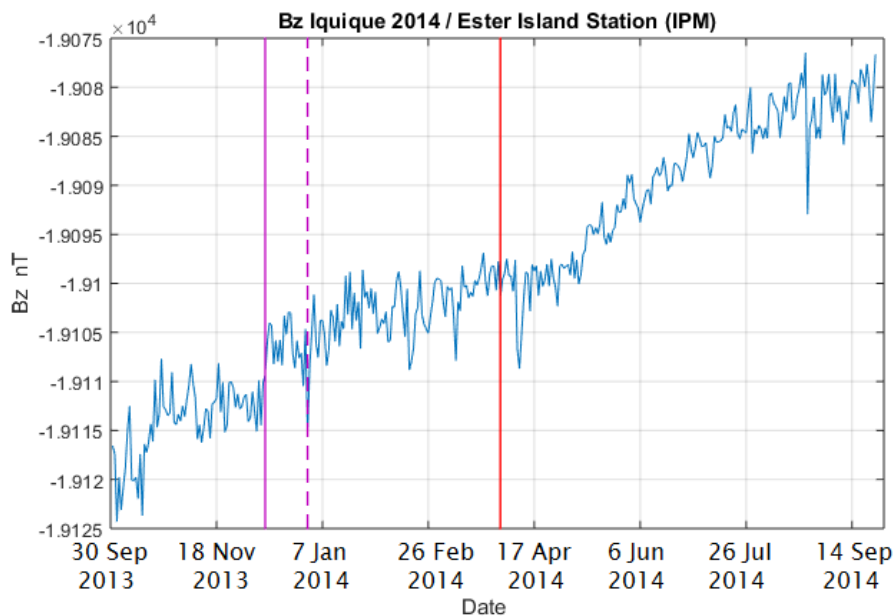
4

5

6

7

8

9

10

1   Figure 6

2
3   Figure 7

4

5

6

7

8

20

Annales
Geophysicae
Discussions

1   Figure 8

Mexico Earthquake Sep/08/2017 Mw8.2
Magnetic anomalies of Y component (first temporal derivative) at Swarm Satallites
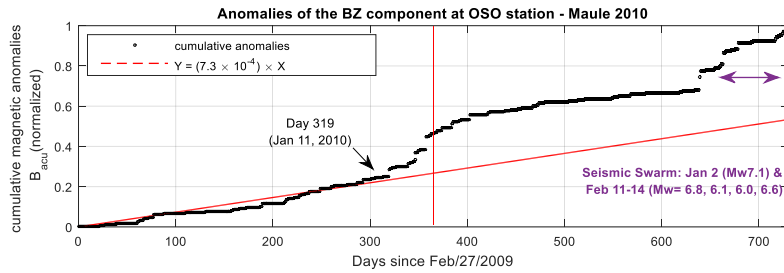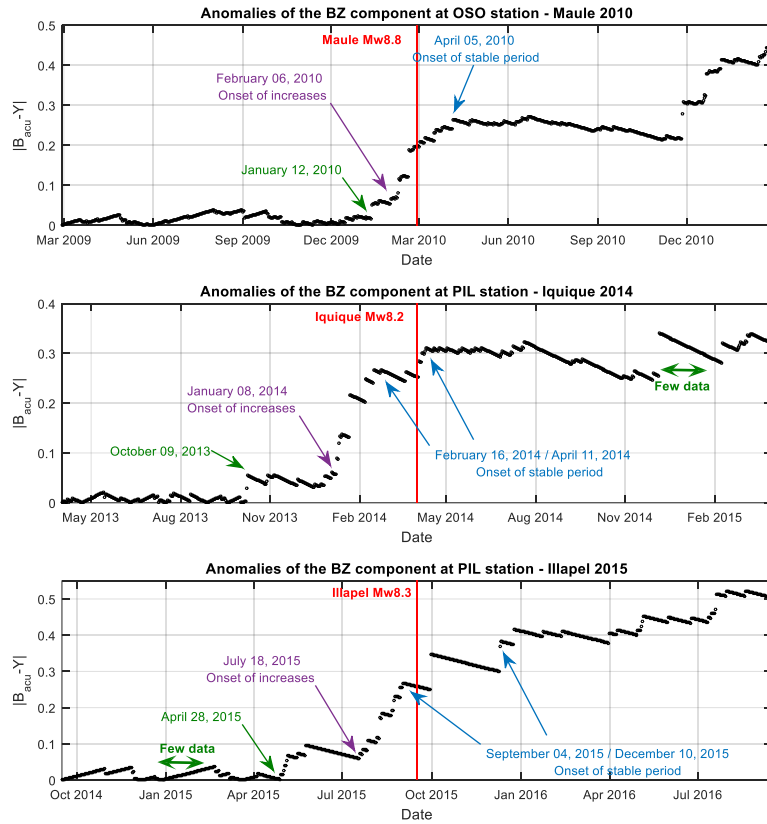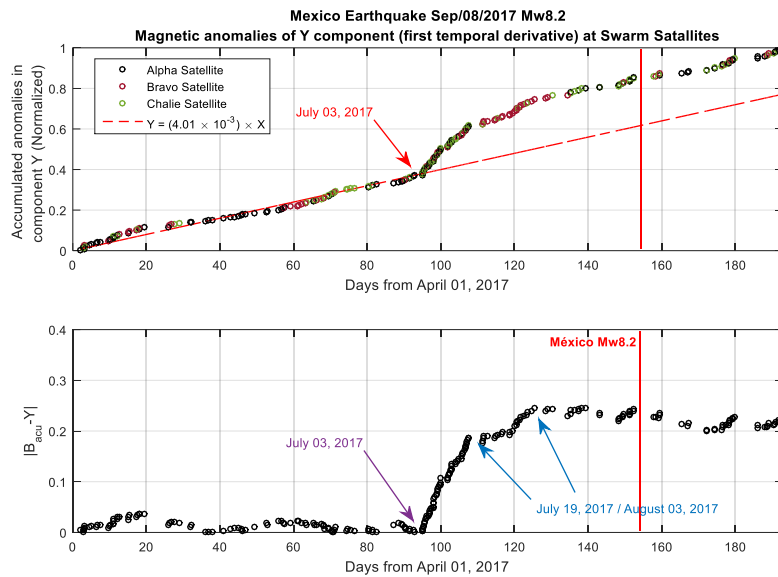
2
3

4

5   Table 1

Observatory	Location	Geographical coordinate	Altitude [m.a.s.l]	Atmospheric Deep [g/cm2]	Instruments	Time
PUTRE (PUT)	Andes Mountain, Chile	18°11´47.8 " S. 69°33´10.9" W	3.600	666	Magnetometer, UCLA-Vectorial-Flux Gate. Muon telescope, 3 channels. Neutron monitor IGY, 3 channels,He 3. UTC by GPS receiver.	2003-2017
Los Cerrillos (OLC)	Santiago de Chile, Chile	33°29´42.2" S. 70°42´59.81 W	570	955	Magnetometer, UCLA-Vectorial-Flux Gate. Multi-dirctional muon telescope, 7 channels. Neutron monitor 6NM64, 3 channels, BF-3. UTC by GPS receiver.	1958-2017
LARC	King George Island, Antarctic	62°12´9"S. 58°57´42¨ W	40	980	Magnetometer, UCLA-Vectorial-Flux Gate. Neutron monitor 6NM64 - BF-3BF-3. 6 channels. Neutron monitor 3NM64 – He-3. 3 channels, Neutron monitor 3NM64 – He-3.[Flux meter] 3 channels. UTC by GPS receiver.	1990-2017

6

7

8   Table 2

Event	Magnitude [Mw]	Radius r [km]	Station Distance from earthquake [km]
Maule 2010	8.8	~6100	Putre ~ 2030
Iquique 2014	8.2	~3360	Putre ~ 300
Illapel 2015	8.3	~3700	IPM ~ 3700

9